# Laminar Flow Friction and Heat Transfer in Non-Circular Ducts and Channels Part I- Hydrodynamic Problem

**Y.S. Muzychka and M.M. Yovanovich**


# Compact Heat Exchangers

**A Festschrift on the 60th Birthday of Ramesh K. Shah**

**Grenoble, France**
**August 24, 2002**

## Proceedings Editors

**G.P. Celata, B. Thonon, A. Bontemps, S. Kandlikar**

**Pages 123-130**

# LAMINAR FLOW FRICTION AND HEAT TRANSFER IN NON-CIRCULAR DUCTS AND CHANNELS PART I - HYDRODYNAMIC PROBLEM

Y.S. Muzychka* and M.M. Yovanovich°

*Faculty of Engineering and Applied Science, Memorial University of Newfoundland, St. John's, NF, Canada, A1B 3X5, °Department of Mechanical Engineering, University of Waterloo, Waterloo, ON, Canada, N2L 3G1

## ABSTRACT

A detailed review and analysis of the hydrodynamic characteristics of laminar developing and fully developed flow in non-circular ducts is presented. New models are proposed which simplify the prediction of the friction factor Reynolds product $fRe$ for developing and fully developed flow in most non-circular duct geometries found in heat exchanger applications. By means of scaling analysis it is shown that complete problem may be easily analyzed by combining the asymptotic results for the short and long duct. Through the introduction of a new characteristic length scale, the square root of cross-sectional area, the effect of duct shape has been minimized. The new model has an accuracy of ± 10 percent or better for most common duct shapes. Both singly and doubly connected ducts are considered.

## NOMENCLATURE

| | | |
|---|---|---|
| $A$ | = | flow area, $m^2$ |
| $a, b$ | = | major and minor axes of ellipse or rectangle, $m$ |
| $C_1, C_2$ | = | constants |
| $c$ | = | linear dimension, $m$ |
| $D$ | = | diameter of circular duct, $m$ |
| $D_h$ | = | hydraulic diameter, $\equiv 4A/P$ |
| $\mathbf{E}(\cdot)$ | = | complete elliptic integral of the second kind |
| $e$ | = | eccentricity, $m$ |
| $e^*$ | = | dimensionless eccentricity, $\equiv e/(r_o - r_i)$ |
| $f$ | = | friction factor $\equiv \tau/(\frac{1}{2}\rho U^2)$ |
| $K$ | = | incremental pressure drop factor |
| $L$ | = | duct length, $m$ |
| $L^+$ | = | dimensionless duct length, $\equiv L/\mathcal{L}Re_{\mathcal{L}}$ |
| $N$ | = | number of sides of a polygon |
| $n$ | = | correlation parameter |
| $P$ | = | perimeter, $m$ |
| $p$ | = | pressure, $N/m^2$ |
| $r$ | = | radius, $m$ |
| $r^*$ | = | dimensionless radius ratio, $\equiv r_i/r_o$ |
| $Re_{\mathcal{L}}$ | = | Reynolds number, $\equiv U\mathcal{L}/\nu$ |
| $\vec{V}$ | = | velocity vector, $m/s$ |
| $u, v, w$ | = | velocity components, $m/s$ |
| $U$ | = | average velocity, $m/s$ |
| $x, y, z$ | = | cartesian coordinates, $m$ |

### *Greek Symbols*

| | | |
|---|---|---|
| $\delta$ | = | boundary layer thickness, $m$ |
| $\epsilon$ | = | aspect ratio, $\equiv b/a$ |
| $\Phi$ | = | half angle, $rad$ |
| $\mu$ | = | dynamic viscosity, $Ns/m^2$ |
| $\rho$ | = | fluid density, $kg/m^3$ |
| $\tau$ | = | wall shear stress, $N/m^2$ |

### *Subscripts*

| | | |
|---|---|---|
| $\sqrt{A}$ | = | based upon the square root of flow area |
| $c$ | = | core |
| $D_h$ | = | based upon the hydraulic diameter |
| $h$ | = | hydrodynamic |
| $i$ | = | inner |
| $\mathcal{L}$ | = | based upon the arbitrary length $\mathcal{L}$ |
| $o$ | = | outer |
| $\infty$ | = | fully developed limit |

### *Superscripts*

| | | |
|---|---|---|
| $C$ | = | circle |
| $E$ | = | ellipse |
| $P$ | = | polygon |
| $R$ | = | rectangle |

## INTRODUCTION

Laminar flow fluid friction and heat transfer in non-circular ducts occurs quite frequently in low Reynolds number flow heat exchangers such as compact heat exchangers. It is now also occurring more frequently in electronic cooling applications as a result of the miniaturization of packaging technologies. While traditional approaches rely heavily on the use of tabulated and/or graphical data, the ability to design thermal systems using robust models is much more desirable. Most modern fluid dynamics and heat transfer texts rarely present correlations or models for more complex geometries which appear in many engineering systems. Rather, a subset of data for miscellaneous geometries is usually presented after detailed discussion and analysis of simple geometries such as the circular duct and parallel plate channel.

In the first part of this paper, the hydrodynamic problem is considered in detail, and a new model is developed for predicting the friction factor Reynolds number product for developing laminar flow in non-circular ducts. In the second part of this paper, the associated thermal problem is considered, and new models are developed for the both

the classic Graetz thermal entrance problem and the combined entrance problem.

Laminar fully developed fluid flow in non-circular ducts of constant cross-sectional area results when the duct length is sufficiently greater than the entrance length, $L >> L_h$, or when the characteristic transversal scale is sufficiently small to ensure a small Reynolds number. Under these conditions the flow through most of the duct may be considered fully developed. In many engineering systems such as compact heat exchangers and micro-coolers used in electronics packaging, the characteristic dimension of the flow channel is small enough to give rise to fully developed flow conditions. However, in many modern systems, the flow length is generally not very large, $L \sim L_h$ or $L << L_h$, and developing flow prevails over most of the duct length. In these situations, a model capable of predicting the hydrodynamic characteristic, usually denoted as $fRe$, the friction factor Reynolds number product, is required.

A review of the literature reveals that only two significant attempts at developing a general model have been undertaken. These are the work of Shah [1] and Yilmaz [2]. These models are based upon the early work of Bender [3]. Bender [3] combined the asymptotic result of Shapiro et al. [4], with the result for the "long" duct, to provide a model which is valid over the entire length of a circular duct. Shah [1] later extended the model of Bender [3] to predict results for the equilateral triangle, the circular annulus, the rectangular duct, and parallel plate channel geometries. Shah [1] achieved this by generalizing the form of the model of Bender [3], and tabulating coefficients for each particular case. Recently, Yilmaz [2] proposed a more general model of Shah [1]. Rather than tabulating coefficients, Yilmaz [2] developed a complex correlation scheme for the fully developed friction factor $fRe$, the incremental pressure drop $K_\infty$, and a fitting coefficient $C$ which appears in the Shah [1] model. This model is more general than that of Shah [1] but is also quite complex.

Despite its complexity, the model of Yilmaz [2] is accurate over the entire range of the entrance and fully developed regions for many duct cross-sections. The primary drawback of the simple model proposed by Shah [1] is the requirement of tabulated coefficients and parameters for each geometry, i.e. $fRe$, $K_\infty$, and $C$, thus limiting interpolation for geometries such as the rectangular duct and circular annulus, whose solution varies with aspect ratio. In the case of the model developed by Yilmaz [2], interpolation is no longer a problem, however, this is achieved at the cost of simplicity.

The two models discussed above represent the current state of the art for internal flow problems. Both models are based upon the combination of the "short" duct and "long" duct solutions using the correlating method of Bender [3]. In this approach the incremental pressure drop factor $K_\infty$ is required in the "long duct" solution. As a result of the complex correlating equations for $K_\infty$ developed by Yilmaz [2], the simple physical behaviour of the hydrodynamic entrance problem is lost. It is apparent from the available data, that smooth transition occurs from the entrance region to that of fully developed flow. Since the solution obtained by Shapiro et al. [4] accounts for the increase in momentum of the accelerating core, use of the term $K_\infty$ in a hydrodynamic entrance model such as that proposed by Bender [3] is redundant. The model presented in this paper does not require this parameter and is significantly simpler in structure.

## GOVERNING EQUATIONS

The governing equations for steady incompressible flow in the hydrodynamic entrance region in a non-circular duct or channel are:

$$\nabla \cdot \vec{V} = 0 \tag{1}$$

$$\rho \vec{V} \cdot \nabla \vec{V} = -\nabla p + \mu \nabla^2 \vec{V} \tag{2}$$

Simultaneous solution to the contiuity, Eq. (1), and momentum, Eq. (2), equations subject to the no slip condiction at the duct wall, $\vec{V} = 0$, the boundedness condition along the duct duct axis, $\vec{V} \neq \infty$, and a constant initial velocity, $\vec{V} = U\vec{k}$, are required to characterize the flow. In the next section, scaling analysis is used to show the appropriate form of the solution for both short and long ducts. Later, asymptotic analysis is used to develop a new model.

## SCALE ANALYSIS

We now examine the momentum equation and consider the various force balances implied under particular flow conditions. The momentum equation represents a balance of three forces: inertia, pressure, and friction, i.e.

$$\underbrace{\rho \vec{V} \cdot \nabla \vec{V}}_{Inertia} = \underbrace{-\nabla p}_{Pressure} + \underbrace{\mu \nabla^2 \vec{V}}_{Friction} \tag{3}$$

We now consider three separate force balances. Each is examined below using the method of scale analysis advocated by Bejan [5].

### Long Duct Asymptote, $\mathbf{L >> L_h}$

Fully developed laminar flow in a duct of arbitrary, but constant cross-section, is governed by the Poisson equation:

$$\underbrace{\nabla p}_{Pressure} = \underbrace{\mu \nabla^2 \vec{V}}_{Friction} \tag{4}$$

which represents a balance between the viscous and pressure forces. Thus we may write the following approximate relation using the characteristics of the flow and the geometry:

$$\frac{\Delta p}{L} \sim \mu \frac{U}{\mathcal{L}^2} \tag{5}$$

where $\mathcal{L}$ represents a characteristic transversal length scale of the duct cross-section. The velocity scales according to the area mean value, $U$, and the axial length scales according to $L$. Rearranging the above expression gives:

$$\Delta p \sim \frac{\mu U L}{\mathcal{L}^2} \tag{6}$$

Next, we examine the shear stress at the wall. The shear stress may be approximated by

$$\vec{\tau} = \mu \nabla \vec{V} \sim \mu \frac{U}{\mathcal{L}} \tag{7}$$

Next, we may introduce the definition of the friction factor defined as the dimensionless wall shear:

$$f \sim \frac{\tau}{\rho U^2} \sim \frac{\mu U/\mathcal{L}}{\rho U^2} \sim \frac{1}{Re_{\mathcal{L}}} \tag{8}$$

The above expression may be written such that the following relationship exists for all cross-sectional geometries:

$$fRe_{\mathcal{L}} \sim \frac{\tau \mathcal{L}}{\mu U} \sim \mathcal{O}(1) \tag{9}$$

or

$$fRe_{\mathcal{L}} = C_1 \tag{10}$$

The constant $C_1$ has been found to vary for most geometries in the range $12 < C_1 < 24$, when $\mathcal{L} = D_h$. Finally, a control volume force balance gives

$$\tau = \frac{\Delta p}{L} \frac{A}{P} \tag{11}$$

yields the following relationship when combined with the two scaling laws, Eqs. (6,7):

$$\mathcal{L} \sim \frac{A}{P} \sim \frac{D_h}{4} \tag{12}$$

We shall see later that this length scale which results from the force balance, although convenient, is not the most appropriate choice.

**Short Duct Asymptote, L << $L_h$**

In the entrance region near the duct inlet two regions must be considered. One is the inviscid core and the other the viscous boundary layer. The flow within the boundary layer is very similar to laminar boundary layer development over a flat plate, except that the velocity at the edge of the boundary layer is not constant. The two regions are now examined beginning with the flow within the boundary layer.

The force balance within the boundary layer is governed strictly by inertia and friction forces:

$$\underbrace{\rho \vec{V} \cdot \nabla \vec{V}}_{Inertia} = \underbrace{\mu \nabla^2 \vec{V}}_{Friction} \tag{13}$$

This balance yields:

$$\rho \frac{U^2}{L} \sim \mu \frac{U}{\delta^2} \tag{14}$$

where $\delta$ is the boundary layer thickness. Thus,

$$\frac{\delta}{L} \sim \frac{1}{\sqrt{Re_L}} \tag{15}$$

Next, considering the relationship for the wall shear:

$$\vec{\tau} = \mu \nabla \vec{V} \sim \mu \frac{U}{\delta} \tag{16}$$

and the friction factor, we obtain:

$$f \sim \frac{\tau}{\rho U^2} \sim \frac{\mu U/\delta}{\rho U^2} \sim \frac{\mu \sqrt{Re_L}}{\rho U L} \sim \frac{1}{\sqrt{Re_L}} \tag{17}$$

Re-writing the above expression in terms of the length scale $\mathcal{L}$, and defining the product of friction factor and Reynolds number yields the following expression for the entrance region:

$$fRe_{\mathcal{L}} \sim \frac{\mathcal{O}(1)}{\sqrt{L^+}} \tag{18}$$

or

$$fRe_{\mathcal{L}} = \frac{C_2}{\sqrt{L^+}} \tag{19}$$

where

$$L^+ = \frac{L}{\mathcal{L} Re_{\mathcal{L}}} \tag{20}$$

is the dimensionless duct length.

Finally, in the inviscid core the momentum equation represents a balance of inertia and pressure forces:

$$\underbrace{\rho \vec{V} \cdot \nabla \vec{V}}_{Inertia} = \underbrace{-\nabla p}_{Pressure} \tag{21}$$

which scales according to

$$\rho U^2 \sim \Delta p \tag{22}$$

Since the pressure at any point along the duct in the developing region must be constant in the core and in the boundary layer, and using the force balance given by Eq. (11), it is not difficult to see that the constant in Eq. (19) will be much larger than the value obtained for boundary layer flow over a flat plate. The constant $C_2$ has been found theoretically [4] for the circular duct to be $C_2 = 3.44$ for a mean friction factor and $C_2 = 1.72$ for a local friction factor.

In summary, we have found from scaling analysis the following relationships for the friction factor Reynolds number product:

$$fRe_{\mathcal{L}} = \begin{cases} C_1 & L >> L_h \\ \dfrac{C_2}{\sqrt{L^+}} & L << L_h \end{cases} \tag{23}$$

This asymptotic behaviour will be examined further and will form the basis for the new model developed for the hydrodynamic entrance problem. Finally, an equation relating the approximate magnitude of the hydrodynamic entrance length may be obtained by considering an equality between the two asymptotic limits given in Eq. (23) with $L^+ = L_h^+$:

$$C_1 = \frac{C_2}{\sqrt{L_h^+}} \tag{24}$$

or

$$L_h^+ = \left( \frac{C_2}{C_1} \right)^2 \tag{25}$$

Later, it will be shown that this approximate scale compares well with more exact solutions. This solution represents the intersection of the asymptotic limits on a plot of the complete behaviour of $fRe$ versus $L^+$.

## ASYMPTOTIC ANALYSIS

In this section, asymptotic analysis [6] is used to establish expressions for the characteristic long duct and short duct behaviour established through scaling analysis. First, the long duct limit is considered and a simple expression developed for predicting the constant $fRe = C_1$. Additionally, the issue of an appropriate characteristic length scale is addressed. Finally, the short duct limit is considered by re-examining the approximate solution obtained by Siegel [7].

### Long Duct Asymptote, L >> $L_h$

In order to establish the long duct limit, solutions to Eq. (4) for many ducts are examined. These solutions have been catalogued in [8,9]. The simplest duct shapes are the circular duct and the parallel plate channel. These important shapes also appear as limits in the elliptical duct, the rectangular duct, and the circular annulus.

One issue which has not been addressed in the literature is the selection of an appropriate characteristic length scale, i.e. $\mathcal{L}$. Traditionally, the hydraulic diameter has been chosen, $\mathcal{L} = 4A/P$. However, in many texts its use in laminar flow has been questioned [10-12]. In an earlier work [13], the authors addressed this issue using dimensional analysis. It was determined that the widely used concept of the hydraulic diameter was inappropriate for laminar flow and the authors proposed using $\mathcal{L} = \sqrt{A}$ as a characteristic length scale, by considering other problems in mathematical physics for which the Poisson equation applies. A more detailed discussion and analysis on the use of $\mathcal{L} = \sqrt{A}$ may be found in Muzychka [14].

We will now examine a number of important results employing both $\mathcal{L} = 4A/P$ and $\mathcal{L} = \sqrt{A}$. Starting with the elliptical duct, the dimensionless average wall shear, Eq. (9), is found to be [8]:

$$fRe_{D_h} = \frac{2\pi(1+\epsilon^2)}{\mathbf{E}(\epsilon')} \tag{26}$$

where $\epsilon = b/a$, the ratio of minor and major axes, and $\epsilon' = \sqrt{1-\epsilon^2}$. Equation (26) has the following limits:

$$fRe_{D_h} = \begin{cases} 16 & \epsilon \to 1 \\ 19.76 & \epsilon \to 0 \end{cases} \tag{27}$$

If the solution is recast using $\mathcal{L} = \sqrt{A}$, as a characteristic length scale, the following relationship is obtained:

$$fRe_{\sqrt{A}} = \frac{2\pi^{3/2}(1+\epsilon^2)}{\sqrt{\epsilon}\mathbf{E}(\epsilon')} \tag{28}$$

Equation (28) has the following limits:

$$fRe_{\sqrt{A}} = \begin{cases} 8\sqrt{\pi} = 14.18 & \epsilon \to 1 \\ \dfrac{2\pi^{3/2}}{\sqrt{\epsilon}} = \dfrac{11.14}{\sqrt{\epsilon}} & \epsilon \to 0 \end{cases} \tag{29}$$

Next, we examine the rectangular duct. The solution for the dimensionless average wall shear [8], considering only the first term of the series gives:

$$fRe_{D_h} = \frac{24}{(1+\epsilon^2)\left[1 - \dfrac{192\epsilon}{\pi^5}\tanh\left(\dfrac{\pi}{2\epsilon}\right)\right]} \tag{30}$$

Equation (30) has the following limits:

$$fRe_{D_h} = \begin{cases} 14.13 & \epsilon \to 1 \\ 24 & \epsilon \to 0 \end{cases} \tag{31}$$

Examination of the single term solution reveals that the greatest error occurs when $\epsilon = 1$, which gives a $fRe$ value 0.7 percent below the exact value of $fRe = 14.23$. Results for a wide range of aspect ratios are tabulated in [8] using a thirty term series which provided seven digit precision.

If the solution is recast using $\mathcal{L} = \sqrt{A}$, as a characteristic length scale, the following expression is obtained:

$$fRe_{\sqrt{A}} = \frac{12}{\sqrt{\epsilon}(1+\epsilon)\left[1 - \dfrac{192\epsilon}{\pi^5}\tanh\left(\dfrac{\pi}{2\epsilon}\right)\right]} \tag{32}$$

Equation (32) has the following limits:

$$fRe_{\sqrt{A}} = \begin{cases} 14.13 & \epsilon \to 1 \\ \dfrac{12}{\sqrt{\epsilon}} & \epsilon \to 0 \end{cases} \tag{33}$$

Table 1 presents a comparison of the exact values [8] with the single term approximation, Eq. (30) and Eq. (32) for both characteristic length scales. Also presented are values which result from using the asymptotic solution for the parallel plate channel. Clearly, this asymyptotic result does an adequate job of predicting the values of $fRe_{\sqrt{A}}$ up to $\epsilon = 0.7$. Beyond this aspect ratio, very little change is observed in the $fRe$ values.

**Table 1**
**Comparison of Single Term Approximation for $fRe$**

| | $fRe_{D_h}$ | | $fRe_{\sqrt{A}}$ | | |
|---|---|---|---|---|---|
| $\epsilon = b/a$ | Exact | Eq. (30) | Exact | Eq. (32) | $12/\sqrt{\epsilon}$ |
| 0.001 | 23.97 | 23.97 | 379.33 | 379.33 | 379.47 |
| 0.01 | 23.68 | 23.68 | 119.56 | 119.56 | 120.00 |
| 0.05 | 22.48 | 22.47 | 52.77 | 52.77 | 53.66 |
| 0.1 | 21.17 | 21.16 | 36.82 | 36.81 | 37.95 |
| 0.2 | 19.07 | 19.06 | 25.59 | 25.57 | 26.83 |
| 0.3 | 17.51 | 17.49 | 20.78 | 20.76 | 21.91 |
| 0.4 | 16.37 | 16.34 | 18.12 | 18.09 | 18.97 |
| 0.5 | 15.55 | 15.51 | 16.49 | 16.46 | 16.97 |
| 0.6 | 14.98 | 14.94 | 15.47 | 15.43 | 15.49 |
| 0.7 | 14.61 | 14.55 | 14.84 | 14.79 | 14.34 |
| 0.8 | 14.38 | 14.31 | 14.47 | 14.40 | 13.42 |
| 0.9 | 14.26 | 14.18 | 14.28 | 14.20 | 12.65 |
| 1 | 14.23 | 14.13 | 14.23 | 14.13 | 12.00 |

Next, a comparison is made between the elliptical and rectangular duct solutions. It is now apparent that the solution for the circular duct and square duct have essentially collapsed to a single value, Eqs. (29, 33). Further, in the limit of small aspect ratio, the results for the elliptic duct and the rectangular duct have also come closer together, Eqs. (29, 33). It is also clear from this analysis, that the square root of cross-sectional area is more appropriate than the hydraulic diameter for non-dimensionalizing the laminar flow data. As seen in Table 2, the maximum difference between the values for $fRe$ occur in the limit of $\epsilon \to 0$. Comparison of Eq. (29) and Eq. (33) shows this difference is only 7.7 percent. Thus, we may use the simpler expression, Eq. (32), to compute values for the elliptical duct. This way, the elliptic integral in Eq. (28) need not be evaluated.

**Table 2**
**$fRe$ Results for Elliptical and Rectangular Geometries [8]**

| | $fRe_{D_h}$ | | | $fRe_{\sqrt{A}}$ | | |
|---|---|---|---|---|---|---|
| $\epsilon = b/a$ | Rect. | Ellip. | $\frac{fRe^R}{fRe^E}$ | Rect. | Ellip. | $\frac{fRe^R}{fRe^E}$ |
| 0.01 | 23.67 | 19.73 | 1.200 | 119.56 | 111.35 | 1.074 |
| 0.05 | 22.48 | 19.60 | 1.147 | 52.77 | 49.69 | 1.062 |
| 0.10 | 21.17 | 19.31 | 1.096 | 36.82 | 35.01 | 1.052 |
| 0.20 | 19.07 | 18.60 | 1.025 | 25.59 | 24.65 | 1.038 |
| 0.30 | 17.51 | 17.90 | 0.978 | 20.78 | 20.21 | 1.028 |
| 0.40 | 16.37 | 17.29 | 0.947 | 18.12 | 17.75 | 1.021 |
| 0.50 | 15.55 | 16.82 | 0.924 | 16.49 | 16.26 | 1.014 |
| 0.60 | 14.98 | 16.48 | 0.909 | 15.47 | 15.32 | 1.010 |
| 0.70 | 14.61 | 16.24 | 0.900 | 14.84 | 14.74 | 1.007 |
| 0.80 | 14.38 | 16.10 | 0.893 | 14.47 | 14.40 | 1.005 |
| 0.90 | 14.26 | 16.02 | 0.890 | 14.28 | 14.23 | 1.004 |
| 1.00 | 14.23 | 16.00 | 0.889 | 14.23 | 14.18 | 1.004 |

**Table 3**
**$fRe$ Results for Polygonal Geometries [8]**

| $N$ | $fRe_{D_h}$ | $\frac{fRe^P}{fRe^C}$ | $fRe_{\sqrt{A}}$ | $\frac{fRe^P}{fRe^C}$ |
|---|---|---|---|---|
| 3 | 13.33 | 0.833 | 15.19 | 1.071 |
| 4 | 14.23 | 0.889 | 14.23 | 1.004 |
| 5 | 14.73 | 0.921 | 14.04 | 0.990 |
| 6 | 15.05 | 0.941 | 14.01 | 0.988 |
| 7 | 15.31 | 0.957 | 14.05 | 0.991 |
| 8 | 15.41 | 0.963 | 14.03 | 0.989 |
| 9 | 15.52 | 0.970 | 14.04 | 0.990 |
| 10 | 15.60 | 0.975 | 14.06 | 0.992 |
| 20 | 15.88 | 0.993 | 14.13 | 0.996 |
| $\infty$ | 16 | 1.000 | 14.18 | 1.000 |

Next, we consider the regular polygons. Values for $fRe_{D_h}$ fall in the range $13.33 \le fRe_{D_h} \le 16$ for $3 \le N \le \infty$. The relative difference between the triangular and the circular ducts is approximately 16.7 percent. When the characteristic length scale is changed to $\mathcal{L} = \sqrt{A}$, the relative difference is reduced to 7.1 percent for the equilateral triangle, and less than 0.1 percent for the remaining polygons. The results are summarized in Table 3. Solutions for a number of other common geometries are shown in Figs. 1 and 2 as a function of aspect ratio. The definition of aspect ratio is summarized in Table 4 for a number of geometries. With the exception of the trapezoid and the annular sector, the aspect ratio for all singly connected ducts is taken as the ratio of the maximum width to maximum length such that $0 < \epsilon < 1$. For the trapezoid, annular sector, and the doubly connected duct, simple expressions have been devised to relate the characteristic dimensions of the duct to a width to length ratio.

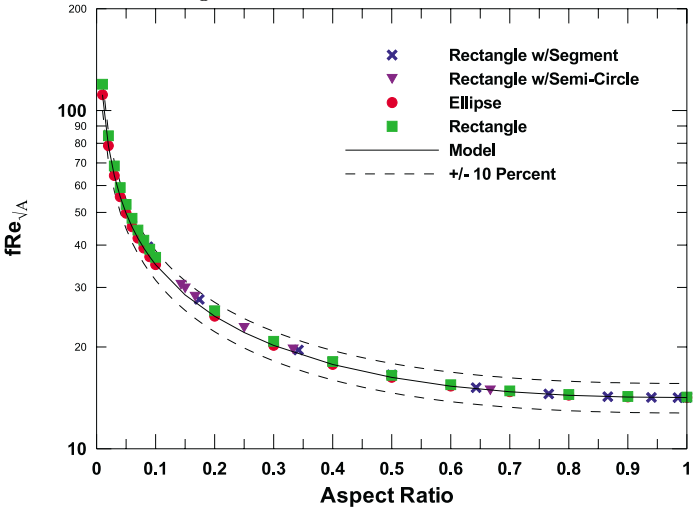


**Fig. 1 - $fRe_{\sqrt{A}}$ for Regular Flat Ducts, Data from Ref. [8]**

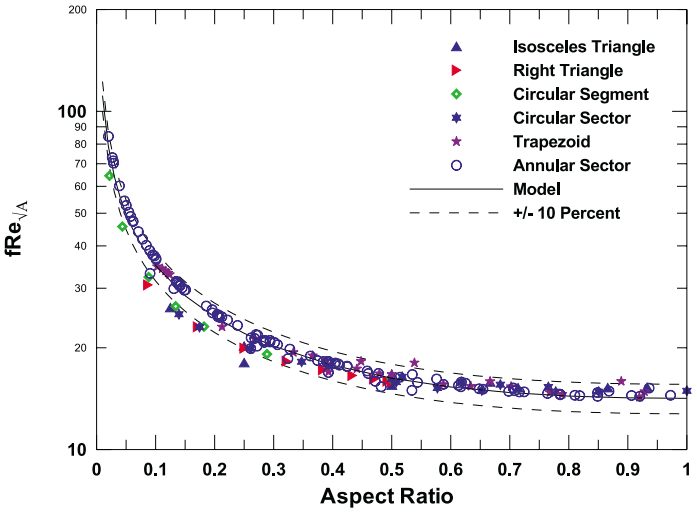


**Fig. 2 - $fRe_{\sqrt{A}}$ for Other Non-Circular Ducts, Data from Ref. [8]**

The final results to be considered are those of the circular annulus and other annular ducts which are bounded externally by a polygon or internally by a polygon [8]. It is clear from Fig. 3 that excellent agreement is obtained when the results are rescaled according to $\mathcal{L} = \sqrt{A}$ and a new aspect ratio defined as $r^* = \sqrt{A_i/A_o}$. This definition was chosen since it returns the same $r^*$ ratio for the circular annular duct. Values for $fRe$ for the circular annulus and other shapes have been examined by Muzychka [14].

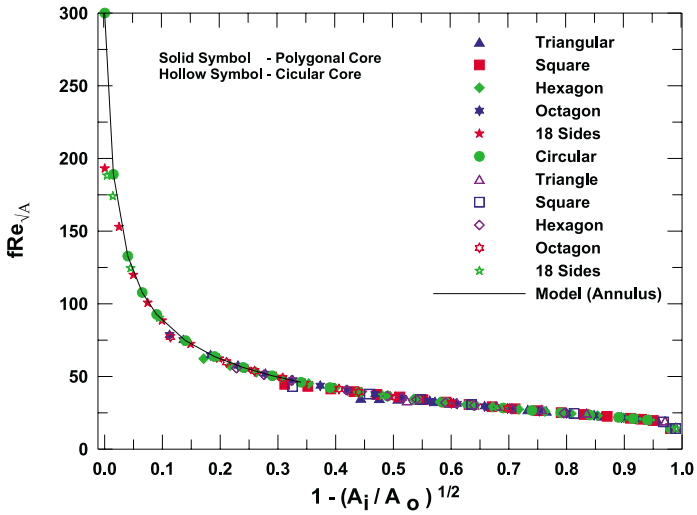


**Fig. 3 - $fRe_{\sqrt{A}}$ for Doubly Connected Ducts, Data from Ref. [8]**

**Table 4**
**Definitions of Aspect Ratio**

| Geometry | Aspect Ratio |
|---|---|
| Regular Polygons | $\epsilon = 1$ |
| Singly-Connected | $\epsilon = \dfrac{b}{a}$ |
| Trapezoid | $\epsilon = \dfrac{2b}{a+c}$ |
| Annular Sector | $\epsilon = \dfrac{1-r^*}{(1+r^*)\Phi}$ |
| Circular Annulus | $\epsilon = \dfrac{(1-r^*)}{\pi(1+r^*)}$ |
| Eccentric Annulus | $\epsilon = \dfrac{(1+e^*)(1-r^*)}{\pi(1+r^*)}$ |

It should be noted that as the inner boundary approaches the outer boundary, there is some departure from the circular annulus result due to the flow field becoming multiply connected. These points have not been shown on the plot. Limiting values of $r^*$ are provided in [13,14]. It has been found that Eq. (32) may be used to predict the results of the circular annulus provided the following equivalent singly connected aspect ratio is defined:

$$\epsilon = \frac{(1-r^*)}{\pi(1+r^*)} \tag{34}$$

This result may be obtained from two different physical arguments. The first is the ratio of the of gap, $r_o - r_i$, to the mean perimeter, while the second is obtained as the ratio of the gap to the equivalent length if the duct area, $\pi(r_o^2 - r_i^2)$, is converted to a rectangle. Both points of view yield the same definition.

It is now clear that Eq. (32) fully characterizes the flow in the long duct limit. The maximum deviation of exact values is of the order 7-10 percent. It has now been shown that the dimensionless average wall shear, $fRe$, may be predicted from Eq. (32), provided an appropriate defintion of the aspect ratio is chosen.

**Short Duct Asymptote, L << $L_h$**

An analytical result for the friction factor in the entrance region of the circular duct was obtained by Siegel [7] using several methods. The solution begins with the definition of the short duct friction factor which may be obtained by writing Bernoulli's equation in the entrance region. Since the pressure gradient is only a function of axial position, the following relationship may be written which relates the friction factor to the velocity in the inviscid core

$$\frac{p_i - p_L}{\frac{1}{2}\rho U^2} = \left(\frac{u_c}{U}\right)^2 - 1 = 4f\left(\frac{L}{D}\right) \tag{35}$$

In order to determine the friction factor, a relationship for the dimensionless core velocity needs to be found. Siegel [7] applied several approximate analytical methods to obtain a solution for the velocity in the inviscid core. The most accurate method was the application of the Method of Thwaites, (see Goldstein [15]). The Siegel [7] analysis begins with the integrated form of the continuity equation in the entance region where the boundary layer is small relative to the duct diameter:

$$\frac{\pi}{4}D^2U = \frac{\pi}{4}(D-2\delta)^2 u_c + \pi\int_0^\delta (D-2y)\,u\,dy \tag{36}$$

where $u$ is the velocity distribution in the boundary layer, $u_c$ is the velocity in the core, and $U$ is the mean velocity. Rearranging this expression leads to

$$\frac{U}{u_c} = 1 - \frac{4}{D}\int_0^\delta \left(1-\frac{u}{u_c}\right)dy + \frac{8}{D^2}\int_0^\delta \left(1-\frac{u}{u_c}\right) y\,dy \tag{37}$$

Next, using Pohlhausen's approximate velocity distribution, Siegel [7] developed an expression relating the boundary layer displacement thickness to the velocity in the core. Siegel [7] then obtained the following four term approximation for the velocity in the core near the entrance of a circular duct

$$\frac{u_c}{U} = 1 + 6.88(L^+)^{1/2} - 43.5(L^+) + 1060(L^+)^{3/2}\cdots \tag{38}$$

Substitution of the above result into the expression for the friction factor yields:

$$fRe_D = \frac{3.44}{(L^+)^{1/2}}\left[1 - 2.88(L^+)^{1/2} + 111(L^+)\cdots\right] \tag{39}$$

Atkinson and Goldstein [15] obtained a solution for the core velocity using a method proposed by Shiller [16] which solves for the velocity in the core using a series expansion. The results of Atkinson and Goldstein [15] yield similar results, with the leading term in the series being exactly the same. A similar analysis for the parallel channel [16] yields the same leading term as that for the circular duct. Analysis of the expressions developed by Siegel [7], and Atkinson

and Goldstein [15], reveal that the leading term may be non-dimensionalized using any characteristic length scale without introduction of scaling terms:

$$fRe_{\mathcal{L}} = \frac{3.44}{(L^+)^{1/2}} \left[ 1 - 2.88(L^+)^{1/2} \left( \frac{\mathcal{L}}{D} \right) + 111(L^+) \left( \frac{\mathcal{L}}{D} \right)^2 \cdots \right] \tag{40}$$

where $L^+$ is defined by Eq. (20).

However, rescaling the additional terms in the expression results in scaling parameters which are now functions of the duct geometry. Thus very near the inlet of any non-circular duct, the leading term of the solution is valid. As the boundary layer begins to grow further downstream, the effects of geometry become more pronounced and the solution for the circular duct is no longer valid. The leading term in the solution for any characteristic length $\mathcal{L}$ is

$$fRe_{\mathcal{L}} = \frac{3.44}{\sqrt{L^+}} \tag{41}$$

which is valid for $L^+ = L/\mathcal{L}\, Re_{\mathcal{L}} \leq 0.001$. If a local friction factor is desired, the constant 3.44 is replaced by 1.72.

Equation (41) is independent of the duct shape and may be used to compute the friction factor for the short duct asymptote of most non-circular ducts.

## MODEL DEVELOPMENT AND COMPARISONS

A general model is now proposed using the Churchill and Usagi [17] asymptotic correlation method. The model takes the form:

$$fRe_{\sqrt{A}} = \left[ (C_1)^n + \left( \frac{C_2}{\sqrt{L^+}} \right)^n \right]^{1/n} \tag{42}$$

where $n$ is a superposition parameter determined by comparison with numerical data over the full range of $L^+$. Using the results provided by Eq. (32) and Eq. (41), and the general expression, Eq. (42), the following model is proposed:

$$fRe_{\sqrt{A}} = \left[ \left( \frac{12}{\sqrt{\epsilon}\,(1+\epsilon) \left[ 1 - \frac{192\epsilon}{\pi^5} \tanh\left( \frac{\pi}{2\epsilon} \right) \right]} \right)^2 + \left( \frac{3.44}{\sqrt{L^+}} \right)^2 \right]^{1/2} \tag{43}$$

Using the available data [8,9], it is found that the value of $n$ which minimizes the root mean square difference lies in the range $1.5 < n < 3.6$ with a mean value $n \approx 2$, [14,18]. Twenty-six data sets were examined from Refs. [8,9] and are summarized in [14,18]. Comparisons of the model are presented in Figs 4-6 for the most common duct shapes. With the exception of the eccentric annular duct at large values of $r^*$ and $e^*$, i.e. a crescent shape, the proposed model predicts all of the developing flow data available in the literature to within ±10 percent or better with few exceptions. The proposed model provides equal or better accuracy than the model of Yilmaz [2] and is also much simpler. A comparison of the model with the data for the parallel plate channel is also provided. For this geometry $\sqrt{A} \to \infty$, however, this geometry may be accurately modeled as a rectangular duct with $\epsilon = 0.01$ or a circular annular duct with $r^* > 0.5$. Good agreement is obtained with the current model when the parallel plate channel is modeled as a finite area duct with small aspect ratio.

One notable feature of the new model is that it does not contain the incremental pressure drop term $K_\infty$ which appears in the models of Bender [3], Shah [1], and Yilmaz [3]. Since the solution of Siegel [7] for the entrance region accounts for both the wall shear and the increase in momentum due to the accelerating core, there is no need to introduce the term $K_\infty$. Thus the proposed model is now only a function of the dimensionless duct length $L^+$ and aspect ratio $\epsilon$, whereas the models of Shah [1] and Yilmaz [2] are functions of many more parameters.

Finally, it is desirable to develop an expression for the hydrodynamic entrance length. Traditionally, the length of hydrodynamic boundary layer development in straight ducts of constant cross-sectional area is usually defined as the point where the centerline velocity is $0.99\,U_{max}$, Shah and London [8]. A new definition for the hydrodynamic entrance length may be obtained from Eq. (25). Substituting Eq. (32) for $C_1$ and $C_2 = 3.44$, an approximate expression for the entrance length is obtained:

$$L_h^+ = 0.0822\epsilon(1+\epsilon)^2 \left[ 1 - \frac{192\epsilon}{\pi^5} \tanh\left( \frac{\pi}{2\epsilon} \right) \right]^2 \tag{44}$$

The expression above reduces to $L_h^+ = 0.059$ when $\epsilon = 1$ and $L_h^+ = 0.00083$ when $\epsilon = 0.01$. These lengths when rescaled to be based on the hydraulic diameter take the values $L_h^+ = 0.047$ when $\epsilon = 1$ and $L_h^+ = 0.021$ when $\epsilon = 0.01$. They compare with the results from Shah and London [8] for the circular duct, $L_h^+ = 0.056$, and parallel plate channel, $L_h^+ = 0.011$.

## SUMMARY AND CONCLUSIONS

A simple model was developed for predicting the friction factor Reynolds number product in non-circular ducts for developing laminar flow. The present study took advantage of scale analysis, asymptotic analysis, and the selection of a more appropriate characteristic length scale to develop a simple model. This model only requires two parameters, the aspect ratio of the duct and the dimensionless duct length. Whereas the model of Shah [1] requires tabulated values of three parameters, and the model of Yilmaz [2] consists of several equations. The present model predicts most of the developing flow data within ± 10 percent or better for 8 singly connected ducts and 2 doubly connected ducts. Finally this model may also be used to predict results for ducts for which no solutions or tabulated data exist. It was also shown that the square root of the cross-sectional flow area was a more effective characteristic length scale than the hydraulic diameter for collapsing the numerical results of geometries having similar shape and aspect ratio.

## ACKNOWLEDGMENTS

The authors acknowledge the financial support of the Natural Sciences and Engineering Research Council of Canada (NSERC).

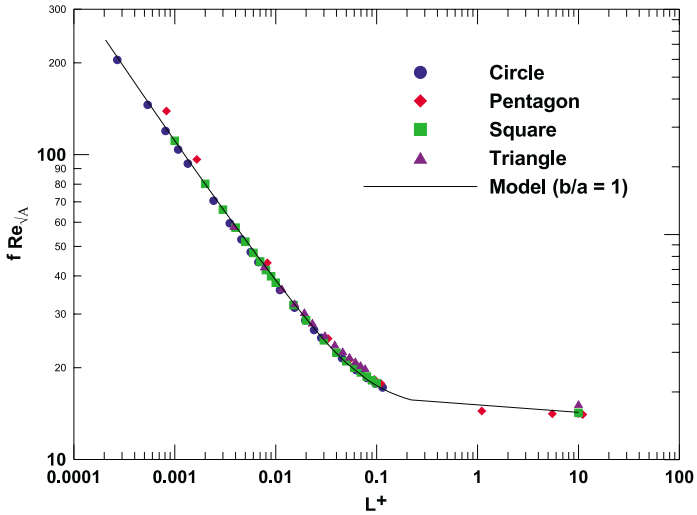


**Fig. 4 - $fRe_{\sqrt{A}}$ for Developing Laminar Flow in Polygonal Ducts, Data from Ref. [8]**

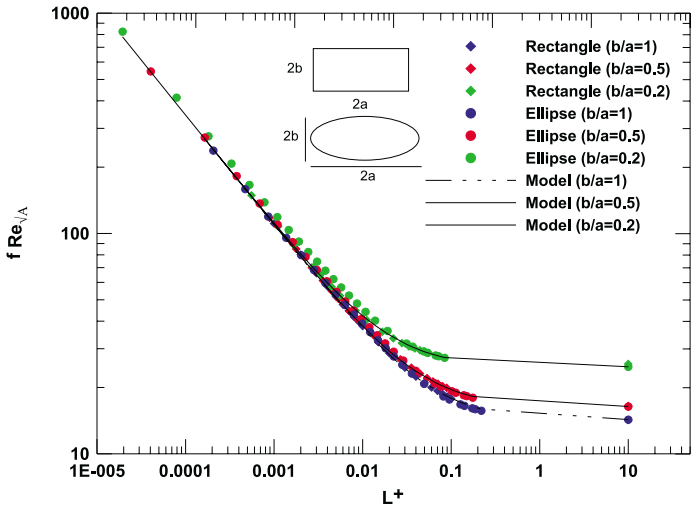


**Fig. 5 - $fRe_{\sqrt{A}}$ for Developing Laminar Flow in Regular Flat Ducts, Data from Ref. [8]**

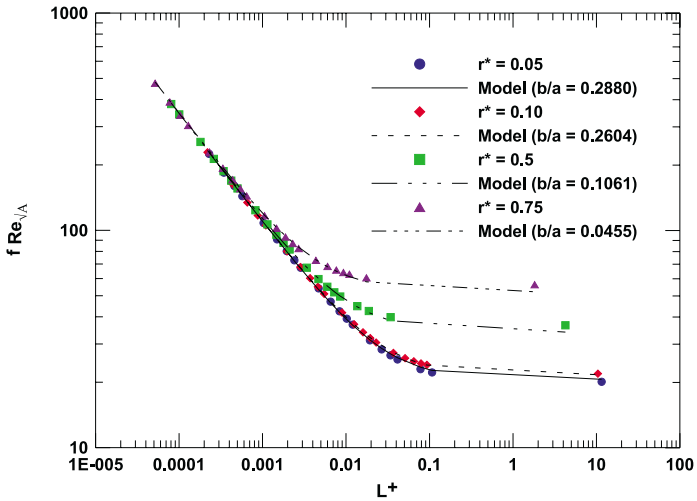


**Fig. 6 - $fRe_{\sqrt{A}}$ for Developing Laminar Flow in the Circular Annular Duct, Data from Ref. [8]**

## REFERENCES


[1] Shah, R. K., "A Correlation for Laminar Hydrodynamic Entry Length Solutions for Circular and Non-Circular Ducts", *Journal of Fluids Engineering*, Vol. 100, 1978, pp. 177-179.

[2] Yilmaz, T., "General Equations for Pressure Drop for Laminar Flow in Ducts of Arbitrary Cross Sections", *Journal of Energy Resources Technology*, Vol. 112, 1990, pp. 220-223.

[3] Bender, E., "Druckverlust bei Laminarer Stromung im Rohreinlauf", *Chemie-Ingenieur Technik*, Vol. 41, 1969, pp. 682-686.

[4] Shapiro, A.H., Siegel, R., and Kline, S.J., " Friction Factor in the Laminar Entry Region of a Smooth Tube", *Proceedings of the 2nd U.S. National Congress of Applied Mechanics*, 1954, pp. 733-741.

[5] Bejan, A., *Convection Heat Transfer, 2nd Ed.*, Wiley, 1995, New York, NY.

[6] Leal, L.G., *Laminar Flow and Convective Transport*, Butterworth-Heinemann, 1992, Boston, MA.

[7] Siegel, R., *The Effect of Heating on Boundary Layer Transition for Liquid FLow in a Tube*, Sc.D. Thesis, 1953, Massachussets Institute of Technology, Boston, MA.

[8] Shah, R.K. and London, A.L., *Laminar Flow Forced Convection in Ducts*, Academic Press, 1978, New York, NY.

[9] Shah, R.K. and Bhatti, M.S., *Chapter 3: Laminar Convective Heat Transfer in Ducts*, in *Handbook of Single Phase Convective Heat Transfer*, eds. S. Kakac, R.K. Shah and W. Aung, Wiley, 1987, New York, NY.

[10] White, F.M., *Viscous Fluid Flow*, McGraw-Hill, 1974, New York, NY.

[11] Denn, M., *Process Fluid Mechanics*, Prentice-Hall, 1980, Upper Saddle River, NJ.

[12] Mironer, A. *Fluid Mechanics*, McGraw-Hill, 1979, New York, NY.

[13] Yovanovich, M.M. and Muzychka, Y.S., "Solutions of Poisson Equation within Singly and Doubly Connected Domains", AIAA 97-3880, *1997 National Heat Transfer Conference*, August 10-12, 1997, Baltimore MD.

[14] Muzychka, Y.S., *Analytical and Experimental Study of Fluid Friction and Heat Transfer in Low Reynolds Number Flow Heat Exchangers*, Ph.D. Thesis, University of Waterloo, 1999, Waterloo, ON.

[15] Goldstein, R. (ed.), *Modern Developments in Fluid Dynamics*, Oxford, 1938, Oxford, UK.

[16] Schlichting, H., *Boundary Layer Theory*, McGraw-Hill, 1979, New York, NY.

[17] Churchill, S. W. and Usagi, R., "A General Expression for the Correlation of Rates of Transfer and Other Phenomena", *American Institute of Chemical Engineers*, Vol. 18, 1972, pp. 1121-1128.

[18] Muzychka, Y.S. and Yovanovich, M.M., "Modelling Friction Factors in Non-Circular Ducts for Developing Laminar Flow", AIAA Paper 98-2492, 2nd *AIAA Theoertical Fluid Mechanics Meeting*, June 15-18, 1998, Albuquerque, NM.